

Comparison of Tungsten Modification After Irradiation at Different Facilities for PSI Studies

Shoshin A.A.^{1,2,a)}, Arakcheev A.S.^{1,2,3}, I.A. Bataev³, V.A. Bataev³,
Burdakov A.V.^{1,3}, Ivanov I.A.^{1,2}, Kasatov A.A.¹, Polosatkin S.V.^{1,2},
Postupaev V.V.^{1,2}, Vasilyev A.A.^{1,2} and Vyacheslavov L.N.^{1,2}

¹ *Budker Institute of Nuclear Physics SB RAS, Novosibirsk, 630090, Russia.*

² *Novosibirsk State University, Novosibirsk, 630090, Russia.*

³ *Novosibirsk State Technical University, Novosibirsk, 630092, Russia.*

^{a)}Corresponding author: shoshin@mail.ru

Abstract. Results from different facilities for plasma-surface interaction (PSI) studies are compared and their relevance to each other and conditions of ITER transient events are discussed. For PSI studies different types of devices were used including open traps, tokamaks, linear plasma machines including quasi-stationary plasma accelerators, electron beams and lasers. The same damage thresholds were demonstrated with different techniques. At energy loads corresponding to ITER transient events (edge localized modes (ELMs), disruptions, etc.) only macroscopic erosion mechanisms are important. They are cracking, droplet formation and macroscopic mass losses of the target. Cracking occurs during cooling stage after irradiations. Details of plasma stream parameters are of secondary importance for cracks formation; only target temperature plays a role. Macroscopic mass losses strongly correspond with melting of a thin surface layer and heat loads play a key role for melting. Heat flux defines the targets surface erosion.

INTRODUCTION

Plasma-surface interaction is one of the main problems of fusion reactors that will affect the performance of ITER and future reactor-type machines. Tungsten is one of the best candidates for the divertor armour material for future fusion devices such as ITER. Unlike carbon materials, tungsten is less prone to tritium capture, but it has a disadvantages of cracking and melting. The energy loads on the ITER divertor surfaces associated with the Type I ELMs are expected to be up to 0.5–10 MJ/m² during 0.1–0.5 ms bursts [1].

TUNGSTEN SURFACE MODIFICATION DEPENDING ON LOAD

Depending on thermal loads, the changes in the tungsten surface modification after an irradiation are different. Under small loads (less than 0.2 MJ/m²), the primary erosion mechanism is physical sputtering, and thus the erosion is acceptably small (after irradiation at the open trap GOL-3 [2] and electron beams facility JUDITH-2 [3]).

Under loads of about 0.5 MJ/m², the tungsten surface did not melt, but after multiple plasma impacts crack patterns are formed (found after irradiation by using Nd:YAG laser [4], [5], quasi-stationary plasma accelerators QSPA Kh-50 [6], linear plasma machines PSI-2 [7], Nd:YAG laser, JUDITH-1 and GOL-3 [8], [9]).

The melting thresholds depend on irradiation conditions and slightly differ for different irradiation methods. At the QSPA Kh-50 plasma gun, a load 0.75 MJ/m² is above the melting threshold [6], but the surface did not melt after electron beam irradiation with the same load [9].

With loads of 1–2 MJ/m² (corresponding to mitigated ITER type I ELMs), the tungsten surface melts, and the loads exceed the evaporation threshold [6]. Bubbles and three different crack networks with typical cell sizes of 1000, 10 and 0.3 μm were detected after irradiation of the tungsten surface by different methods (after irradiation at the Nd:YAG laser [4], QSPA Kh-50 and GOL-3 [6], [10], PSI-2 [7], Nd:YAG laser, JUDITH-1 and GOL-3 [2], [8],

[11]. The typical erosion depth is less than 20 μm [2], [10]. The thickness of the remelted layer was $\sim 35 \mu\text{m}$ [2]. The type of the melted layer fracture can be described as a classic one with low energy of intergranular binding. The main volume of the tungsten sample, which did not undergo melting, shows signs of river patterns, typical of cleavage fracture with areas of intergranular fracture [2]. The newly formed crystals (cell size about 10 μm) have a typical columnar structure of molten material due to intense heat transfer to the internal layers of the tungsten sample. Crack networks with sizes of 0.3 μm are attributed to the formation of individual crystallites [10].

With loads of 4 MJ/m^2 (corresponding to unmitigated ITER type I ELMs), a frozen melt is formed on the tungsten surface instead of crack networks with cell sizes of 1000 μm (GOL-3 [2], [10]). Big droplets, deep bubbles and waves were found on the tungsten surface. The height of the drops after repetitive loads exceeds 200 μm , which demonstrated very large erosion depth for energy density corresponding to the biggest ITER type I ELMs [2], [10].

With loads of 12 MJ/m^2 , the erosion depth after one shot can exceed 200 μm (GOL-3 [12]). The big erosion depth at plasma loads comparable with the lowest estimations of ITER (and DEMO) disruptions and transient events show that big tokamaks have no room for error. Just one unmitigated disruption can lead to a failure in the divertor armor.

TABLE 1. Comparison of different systems for PSI studies.

Type and name	Duration, ms	Loads, MJ/m^2	W cracking and melting thresholds, MJ/m^2
ITER Type I ELMs [1]	0.1–0.5	0.5–10	
Open trap GOL-3 with U-2 accel. [2]	0.01	0.2–30	0.3; 0.9
GOL-3 with long-pulse e-beam [9]	up to 0.3	0.2–3	0.3; 0.9
QSPA-T [13]	0.5	0.3–2	0.2; 1
QSPA Kh-50 [14]	0.25	0.2–2.5	0.3; 0.6
Electron beams facility JUDITH-2 [3]	1	0.2–10	0.25; 1
Nd:YAG laser [4]	1	0.2–1	0.3; 1

CRACKING FORMATION

Cracking formation is one of the most serious problems for tungsten at loads below the melting threshold. Crack network changes the heat conductivity; the resulting melting threshold decreased near cracks. Some cracks can have a large depth (up to several hundred microns) after irradiation at the GOL-3 [2], [9], QSPA Kh-50 [14], JUDITH-2 [3] and laser [15] (see Fig.1). Instead of individual cracks, a crack network was always formed and that can lead to destruction of the material as a whole.

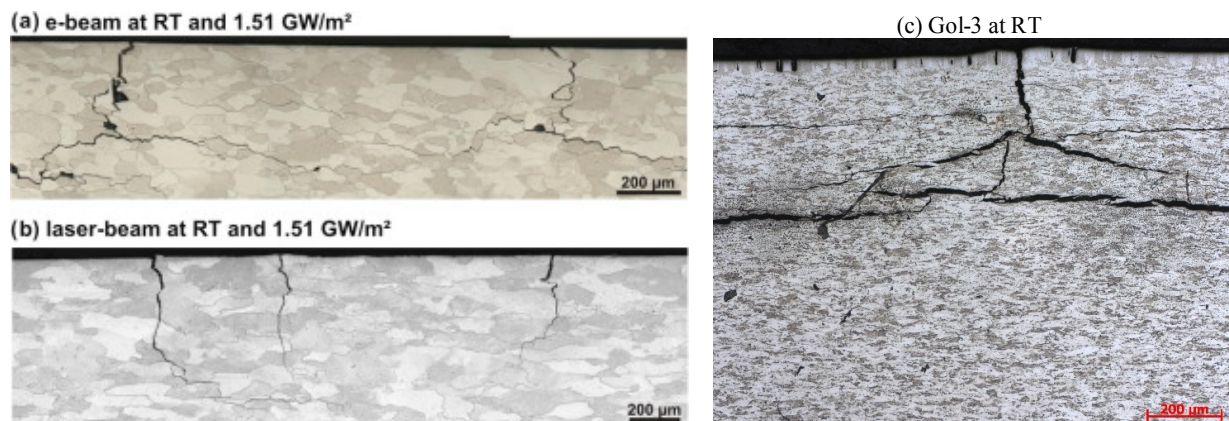


FIGURE 1. Crack propagation in surface layer of irradiated tungsten sample. Transverse microsections of samples irradiated at the JUDITH-1 (a), laser (b) [15] and GOL-3 (c).

The surface cracking increases essentially the surface roughness of tungsten and swelling of the surface profile as a whole relative to the initial reference line. Cracking is a source of tungsten dust, which can deposit in surrounding areas. Horizontal cracking under the surface can decrease the heat transfer to the bulk (Fig.1). During

the irradiation and cooling, this zone (over a crack) can be overheated. In the GOL-3 experiments (by using fast diagnostics [16]), formation of a hot zone on the target surface was revealed (up to 8 ms after irradiation) [9].

Evolution of a crack network (including horizontal cracking) can lead to big cracks and unacceptably large erosion during repetitive irradiations with energy loads corresponding to mitigated ITER ELMs. The cracks can be located a few millimeters below the surface and the surface height difference can be over 1 mm. Cracked parts of target surfaces can produce “dust” of up to several millimeters [9]. Presence of big mobile dust can seriously affect the plasma performance in fusion machines and can decrease the safety threshold for energy loads on PFCs.

The observed typical length of the cracks is about the size of the irradiated surface, which suggests that the local plasma-material interaction is not an immediate cause of the crack formation. The actual reason must be the global mechanical stresses caused by the thermal extension [11].

Analytical calculations of the stresses are carried out for tungsten [11], [17]. The model only takes into account the basic features of solid body mechanics, without material modifications (e.g. fatigue or recrystallization). The following three conditions will be sufficient for explanation of the crack formation: 1) the target temperature exceeds the ductile-to-brittle transition temperature; 2) the maximum value of plastic stress exceeds the ultimate tensile strength; 3) the initial temperature of the target is less than the material-specific threshold. The numerical results of the model demonstrate good agreement with experimental data obtained at the JUDITH-1, PSI-2 and GOL-3 facilities [11], [18]. Experiments show that major cracks (cell size of 1000 μm) are attributed to the ductile-to-brittle transition during cooling stage [9], [19].

DISCUSSION

Let us compare results from different facilities for the PSI studies and discuss their relevance to one another and conditions of ITER transient events. Different irradiation techniques have set of parameters: duration, power loads, surface area, energy and type of particles (photon, electron, ion). This set of parameters is very important for local plasma-surface interaction (for temperature, density and pressure of near surface plasma), but only some of them are important for global surface modification after irradiation.

For example, let us compare irradiation conditions in GOL-3 [20] and QSPA Kh-50 [6], [14]. Parameters of the energy loads of plasma stream for the GOL-3 long pulse accelerator [9], [20], [21] are very close to the QSPA parameters: a pulse duration of up to 0.3 ms and energy loads of up to 2.5 MJ/m². Irradiated surface area in both cases is big enough to use 1D codes and exclude edge effects. After start of plasma irradiation, a vapor shield forms near the target surface. Fast electrons in the GOL-3 facility can easily pass through the vapor shield, so the influence of the shield on the deposited energy is small. At QSPA, the vapor shield effect limits the power delivered to the surface to a level of 4.5 GW/m². Plasma pressure of 2×10^5 Pa in QSPA experiments [22] is at least one order of magnitude larger than that expected for ITER (10^4 Pa) [22] and can result in different mechanisms of droplet ejection in simulations. For example, in the QSPA Kh-50, droplets velocities may achieve several tens of m/s [23], in GOL-3, droplets with velocities of up to several hundred m/s were detected just after the beam termination [24]. The QSPA droplet velocity estimation is undervaluing, and the GOL-3 droplet velocity estimation is overrating because of: 1) the vapor shield pressure in QSPA exceeds that in ITER [22], and the vapor shield pressure in GOL-3 is less than that in ITER; 2) in QSPA, no droplets can be detected during the irradiation and 1 ms after it [25]. The QSPA data about the droplet formation are insufficient, and the GOL-3 data are important for prediction of droplet parameters for ITER transient events. Using an electron beam for heat load simulation is more diagnostics-friendly because the plasma radiation is much lower than in experiments with QSPA, so we were able to observe the dynamics of the target heating and its surface modification, as well as the microparticle ejection starting from the beginning of the heating process [20], [24].

Comparative studies of tungsten targets irradiation with high-power plasma streams generated in GOL-3 and QSPA Kh-50 facilities are being performed [10]. With applied high-energy loads > 1 MJ/m², in spite of qualitative differences in types and energy distribution functions of the bombarding particles, a similar evolution in the surface morphology is observed after the exposures. Thus, the surface heat load plays a key role under high-power plasma impact [10]. The same metal surface modification can be revealed after irradiation by different methods (lasers [26], plasma gun [27], electron beam [28], and QSPA-T [29]).

Moreover, in previous experiments, irradiation at the GOL-3 facility was compared with irradiation using the electron beam facility JUDITH-1 and the Nd:YAG laser [4], [7]. The different techniques show, in general, similar damage behaviour and the same damage thresholds [8], [11].

Why does the heat flux play a key role to the target surface erosion? Under energy loads corresponding to ITER transient events (ELMs, disruptions, etc.), only macroscopic erosion mechanisms are important. They are cracking, droplet formation and macroscopic mass losses in the target, including melting of a thin surface layer, melt motion under the influence of the gravity, pressure gradient and Lorentz forces, evaporation, and vapor shielding. Any of these phenomena is a difficulty, not to mention their interplay.

Recently it was demonstrated that cracking occurs after irradiation, during the cooling stage [9]. So, details of plasma stream parameters and pulse duration are of secondary importance for cracks formation, and the target temperature really matters.

SUMMARY

The analysis of a multi-machine database allows to conclude that the erosion is practically the same with different techniques of target irradiation, because the key role is played by the energy loads.

Does that mean that erosion at the ITER will be the same? No modern plasma machines can exactly reproduce ITER conditions with simultaneous steady-state thermal flux and transient events (with high energy loads) during neutron irradiation in a strong magnetic field with hydrogen and helium fluxes. Most of the effects are synergetic, and it would not be enough just to apply a heat load (or plasma stream) to simulate the ITER conditions. None single machine is relevant to ITER. That is why we need to perform experiments using various techniques of irradiation to collect data about the erosion under different irradiation conditions. Experimental simulation of the ITER type transient heat loads by using different facilities provides important information on the mechanism of tungsten erosion and can be useful for benchmarking of codes.

ACKNOWLEDGMENTS

The work at the GOL-3 facility was supported by the Russian Science Foundation (project No. 14-50-00080). The study of target surface modification was partially supported by the RFBR, research project No. 15-32-20669.

REFERENCES

- [1] A. Loarte, G. Saibene, R. Sartori, V. Riccardo, P. Andrew, J. Paley, W. Fundamenski, T. Eich, A. Herrmann, G. Pautasso, A. Kirk, G. Counsell, G. Federici, G. Strohmayer, D. Whyte, A. Leonard, R.A. Pitts, I. Landman, B. Bazylev, S. Pestchanyi, *Physica Scripta* **T128** (2007) 222-228.
- [2] A.V. Arzhannikov, V.A. Bataev, I.A. Bataev, A.V. Burdakov, I.A. Ivanov, M.V. Ivantsivsky, K.N. Kuklin, K.I. Mekler, A.F. Rovenskikh, S.V. Polosatkin, V.V. Postupaev, S.L. Sinitsky, A.A. Shoshin, *J. Nucl. Mater.* **438** (2013) S677-S680.
- [3] Th. Loewenhoff, J. Linke, G. Pintsuk, C. Thomser, *Fusion Engineering and Design* **87** (7-8) (2012) 1201-1205.
- [4] A. Huber, A. Arakcheev, G. Sergienko, I. Steudel, M. Wirtz, A. V. Burdakov, J. W. Coenen, A. Kreter, J. Linke, Ph. Mertens, V. Philipps, G. Pintsuk, M. Reinhart, U. Samm, A. Shoshin, B. Schweer, B. Unterberg and M. Zlobinski, *Physica Scripta* **T159** (2014) 014005.
- [5] A. Huber, G. Sergienko, M. Wirtz, I. Steudel, A. Arakcheev, S. Brezinsek, A. Burdakov, T. Dittmar, H. G. Esser, A. Kreter, J. Linke, Ch. Linsmeier, Ph. Mertens, S. Moller, V. Philipps, G. Pintsuk, M. Reinhart, B. Schweer, A. Shoshin, A. Terra, B. Unterberg, *Physica Scripta*, **T167** (2016) 014046.
- [6] I.E. Garkusha, A.N. Bandura, O.V. Byrka, V.V. Chebotarev, I. Landman, V.A. Makhilaj, S. Pestchanyi, V.I. Tereshin, *J. Nucl. Mater.* **386-388** (2009) 127-131.
- [7] A. Huber, M. Wirtz, G. Sergienko, I. Steudel, A. Arakcheev, A. Burdakov, G. Esser, M. Freisinger, A. Kreter, J. Linke, C. Linsmeier, P. Mertens, S. Moller, V. Philipps, G. Pintsuk, M. Reinhart, B. Schweer, A. Shoshin, A. Terra, B. Unterberg, *Fusion Engineering and Design* **98-99** (2015) 1328-1332.
- [8] A. Huber, A. Burdakov, M. Zlobinski, M. Wirtz, J. Linke, Ph. Mertens, V. Philipps, G. Pintsuk, B. Schweer, G. Sergienko, A. Shoshin, U. Samm, B. Unterberg, *Fusion Science and Technology* **63** (No.1T) (2013) 197-200.
- [9] A.A. Vasilyev, A.S. Arakcheev, I.A. Bataev, V.A. Bataev, A.V. Burdakov, I.V. Kandaurov, A.A. Kasatov, V.V. Kurkuchekov, K.I. Mekler, V.A. Popov, A.A. Shoshin, D.I. Skovorodin, Yu.A. Trunev,

- L.N. Vyacheslavov, “Observation of the Tungsten Surface Damage under ITER-relevant Transient Heat Loads during and after Electron Beam Pulse”, AIP Conf. Proc. (these proceedings).
- [10] A.A. Shoshin, A.V. Arzhannikov, A.V. Burdakov, V.V. Chebotarev, I.E. Garkusha, I.A. Ivanov, K.N. Kuklin, M.A. Makarov, V.A. Makhraj, A.K. Marchenko, K.I. Mekler, A.F. Rovenskikh, S.V. Polosatkin, V.V. Postupaev, S.L. Sinitsky, V.I. Tereshin, *Fusion Science and Technology* **59** (No.1T) (2011) 57–60.
- [11] A.S. Arakcheev, A. Huber, M. Wirtz, G. Sergienko, I. Steudel, A.V. Burdakov, J.W. Coenen, A. Kreter, J. Linke, Ph. Mertens, A.A. Shoshin, B. Unterberg, A.A. Vasilyev, *J. Nucl. Mater.* **463** (2015) 246–249.
- [12] V.T. Astrelin, A.V. Burdakov, P.Z. Chebotarev, V.V. Filippov, V.S. Koidan, K.I. Mekler, P.I. Melnikov, V.V. Postupaev, A.F. Rovenskikh, M.A. Schcheglov and H. Wurz, *Nuclear Fusion* **37** (11) (1997), 1541-1558.
- [13] K. Wittlich, T. Hirai, J. Compan, N. Klimov, J. Linke, A. Loarte, M. Merola, G. Pintsuk, V. Podkovyrov, L. Singheiser, A. Zhitlukhin, *Fusion Engineering and Design* **84** (2009) 1982–1986.
- [14] I.E. Garkusha, N.I. Arkhipov, N.S. Klimov, V.A. Makhraj, V.M. Safronov, I. Landman, V.I. Tereshin, *Physica Scripta* **T138** (2009) 14054.
- [15] M. Wirtz, J. Linke, G. Pintsuk, L. Singheiser, M. Zlobinski, *J. Nucl. Mater.* **438** (2013) S833–S836.
- [16] A.A. Ivanova, P.V. Zubarev, S.V. Ivanenko, A.N. Kvashnin, D.V. Moiseev, A.I. Kotelnikov, E.A. Puryga, A.D. Khilchenko, V.A. Khilchenko, V.G. Shvyrev, *INSTRUM EXP TECH+* **59**(3), 344–350 (2016).
- [17] A.S. Arakcheev, A.V. Burdakov, A. Huber, A.A. Kasatov, A. Kreter, Ch. Linsmeier, Th. Lowenhoff, Ph. Mertens, A.A. Shoshin, D.I. Skovorodin, A.A. Vasilyev, L.N. Vyacheslavov and M. Wirtz, “Modeling of Crack Formation after Pulse Heat Load in ITER-grade Tungsten”, AIP Conf. Proc. (these proceedings).
- [18] A.S. Arakcheev, D.I. Skovorodin, A.V. Burdakov, A.A. Shoshin, S.V. Polosatkin, A.A. Vasilyev, V.V. Postupaev, L.N. Vyacheslavov, A.A. Kasatov, A. Huber, Ph. Mertens, M. Wirtz, Ch. Linsmeier, A. Kreter, Th. Lowenhoff, L. Begrambekov, A. Grunin, Ya. Sadovskiy, *J. Nucl. Mater.* **467** Part 1, 165-171 (2015).
- [19] A.S. Arakcheev, A.I. Ancharov, V.M. Aulchenko, S.V. Bugaev, A.V. Burdakov, A.D. Chernyakin, O.V. Evdokov, I.V. Kandaurov, A.A. Kasatov, V.S. Koidan, A.V. Kosov, B.I. Khripunov, V.V. Kurkuchekov, P.A. Piminov, S.V. Polosatkin, V.A. Popov, M.R. Sharafutdinov, L.I. Shekhtman, A.N. Shmakov, A.A. Shoshin, D.I. Skovorodin, I.N. Skovorodin, B.P. Tolochko, Y.A. Trunev, A.A. Vasilyev, L.N. Vyacheslavov and V.V. Zhulanov, “Applications of Synchrotron Radiation Scattering to Studies of Plasma Facing Components at Siberian Synchrotron and Terahertz Radiation Centre”, AIP Conf. Proc. (these proceedings)
- [20] L. Vyacheslavov, A. Arakcheev, A. Burdakov, I. Kandaurov, A. Kasatov, V. Kurkuchekov, K. Mekler, V. Popov, A. Shoshin, D. Skovorodin, Y. Trunev, A. Vasilyev, “Novel Electron Beam Based Test Facility for Observation of Dynamics of Tungsten Erosion under Intense ELM-like Heat Loads”, AIP Conf. Proc. (these proceedings).
- [21] Yu.A. Trunev, A.S. Arakcheev, A.V. Burdakov, I.V. Kandaurov, A.A. Kasatov, V.V. Kurkuchekov, K.I. Mekler, V.A. Popov, A.A. Shoshin, D.I. Skovorodin, A.A. Vasilyev, L.N. Vyacheslavov, “Heating of tungsten target by intense pulse electron beam”, AIP Conf. Proc. (these proceedings).
- [22] J.W. Coenen, V. Philipps, S. Brezinsek, B. Bazylev, A. Kreter, T. Hirai, M. Laengner, T. Tanabe, Y. Ueda, U. Samm, *Nucl. Fusion* **51** (2011) 083008 (11pp).
- [23] I.E. Garkusha, V.A. Makhraj, V.V. Chebotarev, I. Landman, V.I. Tereshin, N.N. Aksenov, A.N. Bandura, *J. Nucl. Mater.* **390–391** (2009) 814–817.
- [24] A.A. Kasatov, A.S. Arakcheev, A.V. Burdakov, I.V. Kandaurov, V.V. Kurkuchekov, V.A. Popov, A.A. Shoshin, D.I. Skovorodin, Yu.A. Trunev, A.A. Vasilyev and L.N. Vyacheslavov, “Observation of Dust Particles Ejected from Tungsten Surface under Impact of Intense Transient Heat Load”, AIP Conf. Proc. (these proceedings).
- [25] N. Klimov, V. Podkovyrov, A. Zhitlukhin, D. Kovalenko, B. Bazylev, G. Janeschitz, I. Landman, S. Pestchanyi, G. Federici, A. Loarte, M. Merola, J. Linke, T. Hirai, J. Compan, *J. Nucl. Mater.* **390–391** (2009) 721–726.
- [26] A. Suslova, O. El-Atwani, S.S. Harilal and A. Hassanein *Nuclear Fusion* **55** (2015) 033007.
- [27] A. V. Ankudinov, A. V. Voronin, V. K. Gusev, Ya. A. Gerasimenko, E. V. Demina, M. D. Prusakova, and Yu. V. Sud’enkov *Technical Physics* **59** (3) (2014) 346-352.
- [28] X. Liu, Y. Lian, L. Chen, Z. Chen, J. Chen, X. Duan, J. Fan, J. Song, *J. Nucl. Mater.* **463** (2015) 166-169.
- [29] V.P. Budaev, Y.V. Martynenko, L.N. Khimchenko, A.M. Zhitlukhin, N.S. Klimov, R.A. Pitts, J. Linke, B. Bazylev, N.E. Belova, A.V. Karpov, D.V. Kovalenko, V.L. Podkovyrov, A.D. Yaroshevskaya, *Plasma Physics Reports* **39** (11) (2013) 910-924.